Dimensional effects on exciton states in nanorings

2007 J. Phys.: Condens. Matter 19 346202

(http://iopscience.iop.org/0953-8984/19/34/346202)

IOP PUBLISHING JOURNAL OF PHYSICS: CONDENSED MATTER

J. Phys.: Condens. Matter **19** (2007) 346202 (11pp) doi:10.1088/0953-8984/19/34/346202

Dimensional effects on exciton states in nanorings

Zhensheng Dai and Jia-Lin Zhu

Department of Physics, Tsinghua University, Beijing 100084, People's Republic of China

E-mail: zjl-dmp@mail.tsinghua.edu.cn

Received 12 April 2007, in final form 21 June 2007
Published 20 July 2007
Online at stacks.iop.org/JPhysCM/19/346202

Abstract

Exciton states in nanorings are studied within the framework of the effective-mass approximation. The exciton level structure and binding energy in one- and two-dimensional nanorings are found to be very different at small and large radius limits. The variation of exciton energy levels with radius and width is shown. The important role of Coulomb interaction in exciton spectra is revealed. Our study is helpful for understanding the transition of exciton states from the one-dimensional case to the two-dimensional case.

(Some figures in this article are in colour only in the electronic version)

1. Introduction

Rapid development in fabrication techniques has made it possible to realize nanoscopic semiconductor rings [1–4]. Because of their special shape and size (60–100 nm in outer diameter, about 20 nm in inner diameter and 2 nm in height) [3], carriers can be well confined in three dimensions and can propagate coherently. In experiments, many spectroscopic techniques have been used to investigate the properties of nanorings. Capacitance–voltage spectroscopy measurements show that only one or two electrons can be filled in the ring, and far-infrared transmission spectroscopy under a magnetic field shows the transition of the ground state from angular momentum $l = 0$ to -1 [3, 4]. Photoluminescence (PL) spectra of nanorings have also been measured to investigate the energy-level structures of neutral and charged excitons [5–9]. In theoretical studies, various potential models and methods have been used to study the abundant electronic structure of carriers in nanorings [10–21]. The Aharonov–Bohm (AB) oscillations of excitonic levels have been predicted in a one-dimensional (1D) nanoring [22–24]. Yet, there are still controversies over whether the AB effect of excitons exists or whether it can be observed in realistic nanorings [25–35]. Recently, studies of polarized excitons and their optical AB effect in nanorings have been presented [36, 37].

Quantum behaviours of excitons in nanorings, such as AB effects, are strongly related to the ring dimension and Coulomb interaction [38, 39]. However, only a few groups have concentrated on the effects of dimension and interaction on energy spectra of excitons in nanorings [38–41]. More effort is still needed to get a better understanding of the difference of

excitonic properties in nanorings of different dimensions. The difference of energy levels and binding energies between 1D and two-dimensional (2D) nanorings, as well as the transition between them, has not been systematically studied. In this paper, we investigate the energy levels and binding energies of exciton states in 1D, quasi-1D (Q1D) and 2D nanorings. The dimensional effects on energy levels and singularity effects on wavefunctions are also discussed. The remainder of this paper is organized as follows. The model Hamiltonian and calculation method are presented in section 2. Energy levels and binding energies of an exciton in different nanorings are discussed in section 3. Finally, we summarize our results in section 4. The variation–diagonalization (V–D) method we use is described in the appendix.

2. The model

The Hamiltonian of an exciton confined in a 2D nanoring with radius R and width W can be written as

$$H = \sum_{i=\mathrm{e,h}} \left[-\frac{\hbar^2}{2m_i^*}\nabla_i^2 + U_i\left(r_i\right) \right] - \frac{\omega e^2}{4\pi\epsilon_0\epsilon_\mathrm{r}\left|\vec{r}_\mathrm{e} - \vec{r}_\mathrm{h}\right|}, \tag{1}$$

where ω is adopted to indicate whether the Coulomb interaction term is included ($\omega = 1$) or not ($\omega = 0$). $m_{\mathrm{e(h)}}$ and $U_{\mathrm{e(h)}}$ are the effective mass and corresponding ring-like potential for electrons (holes). ϵ_0 and ϵ_r are the vacuum permittivity and static dielectric constant of the host material, respectively. In the following calculations, the confinement is modelled by an infinite hard-wall potential with radius R and width W. R and W are respectively defined as the average value of the inner and outer radius and their difference. When W is much smaller than R and a_B (the effective Bohr radius of excitons), the nanoring is usually regarded as a Q1D case. $W = 0$ corresponds to so-called 1D nanorings.

The confinement of radial motion is always stronger than that of azimuthal motion, which is much more easily affected by Coulomb interaction. We can adiabatically separate the Hamiltonian of equation (1) into two parts, as follows:

$$H = H_\mathrm{R} + H_\mathrm{A} \tag{2}$$

with

$$H_\mathrm{R} = \sum_{i=\mathrm{e,h}} \left[-\frac{\hbar^2}{2m_i^*}\left(\frac{\partial^2}{\partial r_i^2} + \frac{1}{r_i}\frac{\partial}{\partial r_i}\right) + U_i(r_i) \right] \tag{3}$$

and

$$H_\mathrm{A} = -\frac{\hbar^2}{2m_\mathrm{e}^* r_\mathrm{e}^2}\frac{\partial^2}{\partial\varphi_\mathrm{e}^2} - \frac{\hbar^2}{2m_\mathrm{h}^* r_\mathrm{h}^2}\frac{\partial^2}{\partial\varphi_\mathrm{h}^2} - \frac{\omega e^2}{4\pi\epsilon_0\epsilon_\mathrm{r}\sqrt{r_\mathrm{e}^2 + r_\mathrm{h}^2 - 2r_\mathrm{e}r_\mathrm{h}\cos\left(\varphi_\mathrm{e} - \varphi_\mathrm{h}\right)}}. \tag{4}$$

H_A includes both the azimuthal motion part and a Coulomb interaction term. In terms of center-of-mass coordinate $\Theta = (m_\mathrm{e}^*\varphi_\mathrm{e} + m_\mathrm{h}^*\varphi_\mathrm{h})/(m_\mathrm{e}^* + m_\mathrm{h}^*)$ and relative coordinate $\varphi = \varphi_\mathrm{e} - \varphi_\mathrm{h}$, H_A can be expressed as

$$H_\mathrm{A} = H_\mathrm{Ac} + H_\mathrm{Ar} + H_\mathrm{A}', \tag{5}$$

with

$$H_\mathrm{Ac} = -\frac{\hbar^2}{2\left(m_\mathrm{e}^* + m_\mathrm{h}^*\right)^2}\left(\frac{m_\mathrm{e}^*}{r_\mathrm{e}^2} + \frac{m_\mathrm{h}^*}{r_\mathrm{h}^2}\right)\frac{\partial^2}{\partial\Theta^2}, \tag{6}$$

$$H_\mathrm{Ar} = -\frac{\hbar^2}{2}\left(\frac{1}{m_\mathrm{e}^* r_\mathrm{e}^2} + \frac{1}{m_\mathrm{h}^* r_\mathrm{h}^2}\right)\frac{\partial^2}{\partial\varphi^2} - \frac{\omega e^2}{4\pi\epsilon_0\epsilon_\mathrm{r}\sqrt{r_\mathrm{e}^2 + r_\mathrm{h}^2 - 2r_\mathrm{e}r_\mathrm{h}\cos\left(\varphi\right)}}, \tag{7}$$

and

$$H'_{\mathrm{A}} = -\frac{\hbar^2}{\left(m_{\mathrm{e}}^* + m_{\mathrm{h}}^*\right)}\left(\frac{1}{r_{\mathrm{e}}^2} - \frac{1}{r_{\mathrm{h}}^2}\right)\frac{\partial}{\partial\Theta}\frac{\partial}{\partial\varphi}. \tag{8}$$

In order to solve H_{A} numerically, we introduce variational parameters R_{e}, R_{h}, Δ and δ to describe the effective $\langle r_{\mathrm{e}}\rangle$, $\langle r_{\mathrm{h}}\rangle$, $\langle\sqrt{r_{\mathrm{e}}^2 + r_{\mathrm{h}}^2}\rangle$, $\langle(2r_{\mathrm{e}}r_{\mathrm{h}})/(r_{\mathrm{e}}^2 + r_{\mathrm{h}}^2)\rangle$, respectively. Then H_{A} is rewritten as

$$H_{\mathrm{A}} = H_{\mathrm{Q}} + H'_{\mathrm{Q}} \tag{9}$$

with

$$H_{\mathrm{Q}} = H_{\mathrm{Qc}} + H_{\mathrm{Qr}}, \tag{10}$$

where

$$H_{\mathrm{Qc}} = -\frac{\hbar^2}{2\left(m_{\mathrm{e}}^* + m_{\mathrm{h}}^*\right)^2}\left(\frac{m_{\mathrm{e}}^*}{R_{\mathrm{e}}^2} + \frac{m_{\mathrm{h}}^*}{R_{\mathrm{h}}^2}\right)\frac{\partial^2}{\partial\Theta^2}, \tag{11}$$

$$H_{\mathrm{Qr}} = -\frac{\hbar^2}{2}\left(\frac{1}{m_{\mathrm{e}}^* R_{\mathrm{e}}^2} + \frac{1}{m_{\mathrm{h}}^* R_{\mathrm{h}}^2}\right)\frac{\partial^2}{\partial\varphi^2} - \frac{\omega e^2}{4\pi\epsilon_0\epsilon_{\mathrm{r}}\Delta\sqrt{1-\delta\cos(\varphi)}}, \tag{12}$$

and $H_{\mathrm{Q}'}$ is the remainder of H_{A}.

Equation (3) can be exactly solved by a series expansion method [10]. Its eigenvalues and corresponding eigenfunctions are given as $E_{\mathrm{R}}(n_{\mathrm{e}}) + E_{\mathrm{R}}(n_{\mathrm{h}})$ and $\Psi_{\mathrm{R},n_{\mathrm{e}}}(r_{\mathrm{e}})\Psi_{\mathrm{R},n_{\mathrm{h}}}(r_{\mathrm{h}})$. Since those variational parameters in equations (11) and (12) could be different for different n_{e} and n_{h}, we replace them with $R_{n_{\mathrm{e}}}^{\mathrm{e}}$, $R_{n_{\mathrm{h}}}^{\mathrm{h}}$, $\Delta_{n_{\mathrm{e}},n_{\mathrm{h}}}$ and $\delta_{n_{\mathrm{e}},n_{\mathrm{h}}}$, respectively, to better describe the Coulomb interaction. The eigenfunctions of equation (10) can be written as the product of $\Psi_{\mathrm{Qc}}(\Theta)$ and $\Psi_{\mathrm{Qr}}(\varphi)$. Noting the periodic boundary conditions of φ_{e} and φ_{h}, i.e., $\Psi_{\mathrm{Q}}(\varphi_{\mathrm{e}},\varphi_{\mathrm{h}}) = \Psi_{\mathrm{Q}}(\varphi_{\mathrm{e}}+2\pi,\varphi_{\mathrm{h}}) = \Psi_{\mathrm{Q}}(\varphi_{\mathrm{e}},\varphi_{\mathrm{h}}+2\pi)$, we can deduce both the period of $\Psi_{\mathrm{Qc}}(\Theta)$ to be 2π, and the following relation

$$\Psi_{\mathrm{Qc}}(\Theta)\Psi_{\mathrm{Qr}}(\varphi) = \Psi_{\mathrm{Qc}}\left(\Theta + \frac{2\pi m_{\mathrm{e}}^*}{m_{\mathrm{e}}^* + m_{\mathrm{h}}^*}\right)\Psi_{\mathrm{Qr}}(\varphi + 2\pi). \tag{13}$$

Equation (11) can be simply solved as

$$\begin{aligned} E_{\mathrm{Qc}}(M) &= \frac{\hbar^2 M^2}{2\left(m_{\mathrm{e}}^* + m_{\mathrm{h}}^*\right)^2}\left(\frac{m_{\mathrm{e}}^*}{R_{n_{\mathrm{e}}}^{\mathrm{e}\,2}} + \frac{m_{\mathrm{h}}^*}{R_{n_{\mathrm{h}}}^{\mathrm{h}\,2}}\right) \\ \Psi_{\mathrm{Qc},M}(\Theta) &= \frac{1}{\sqrt{2\pi}}\exp(\mathbf{i}M\Theta) \end{aligned} \tag{14}$$

with $M = 0, \pm1, \pm2, \ldots$. Then the solution to equation (13) is

$$\Psi_{\mathrm{Qr}}(\varphi) = \exp\left(\frac{\mathbf{i}2M\pi m_{\mathrm{e}}^*}{m_{\mathrm{e}}^* + m_{\mathrm{h}}^*}\right)\Psi_{\mathrm{Qr}}(\varphi + 2\pi). \tag{15}$$

The eigenenergies $E_{\mathrm{Qr}}(j)$ and eigenfunctions $\Psi_{\mathrm{Qr},j}(\varphi)$ of equation (12) including Coulomb interaction ($\omega = 1$) can be obtained by using a series expansion method [42] with $j = 0, 1, 2, \ldots$ indicating the order of energy levels. Based on the above solutions, a set of variational bases can be constructed as

$$\Psi_\lambda = \Psi_{R,n_{\mathrm{e}}}(r_{\mathrm{e}})\Psi_{R,n_{\mathrm{h}}}(r_{\mathrm{h}})\Psi_{\mathrm{Qc},M}(\Theta)\Psi_{\mathrm{Qr},j}(\varphi), \tag{16}$$

where $\lambda = \{n_{\mathrm{e}}, n_{\mathrm{h}}, M, j\}$ represents the set of quantum numbers defined above. By defining

$$E_\lambda = E_{\mathrm{R}}(n_{\mathrm{e}}) + E_{\mathrm{R}}(n_{\mathrm{h}}) + E_{\mathrm{Qc}}(M) + E_{\mathrm{Qr}}(j) \tag{17}$$

$$H'_{\mathrm{Q},\lambda,\lambda'} = \langle\lambda|H'_{\mathrm{Q}}|\lambda\rangle, \tag{18}$$

the V–D process, which will be described explicitly in the appendix, can be simply written as

$$\begin{aligned}&\sum_{\lambda'}[(E_\lambda - E_i)\delta_{\lambda,\lambda'} + \mathcal{H}'_{\mathrm{Q},\lambda,\lambda'}]A^i_{\lambda'} = 0\\ &E_\mathrm{g} = \min_{\{R^\mathrm{e}_{n_\mathrm{e}}, R^\mathrm{h}_{n_\mathrm{h}}, \Delta_{n_\mathrm{e},n_\mathrm{h}}, \delta_{n_\mathrm{e},n_\mathrm{h}}\}} E_0.\end{aligned} \tag{19}$$

The eigenenergies E_i, including $E_\mathrm{g} = E_0$, and the expansion coefficients of the eigenwavefunctions $A^i_{\lambda'}$ can be simultaneously obtained with proper parameters.

Without Coulomb interaction ($\omega = 0$), equation (12) is analytically solvable.

$$\begin{aligned}&E_{\mathrm{Qr}}(m) = \frac{\hbar^2 m^2}{2}\left(\frac{1}{m^*_\mathrm{e} R^{\mathrm{e}\,2}_{n_\mathrm{e}}} + \frac{1}{m^*_\mathrm{h} R^{\mathrm{h}\,2}_{n_\mathrm{h}}}\right)\\ &\Psi_{\mathrm{Qr},m}(\varphi) = \frac{1}{\sqrt{2\pi}}\exp(\mathbf{i}m\varphi),\end{aligned} \tag{20}$$

where $m = k - (Mm^*_\mathrm{e})/(m^*_\mathrm{e} + m^*_\mathrm{h})$ with k an integer. The process of obtaining eigenenergies and wavefunctions is similar to that in the $\omega = 1$ case. However, the quantum number j there should be replaced by k. Then the binding energy of ground state can be obtained as

$$E_\mathrm{B} = E_\mathrm{g}(\omega = 0) - E_\mathrm{g}(\omega = 1). \tag{21}$$

What has been introduced above is for 2D nanorings. For a Q1D nanoring, the radial motion of the electron and the hole can be approximately decoupled from the azimuthal motion due to the small width. Thus, $R^\mathrm{e}_{n_\mathrm{e}}$ and $R^\mathrm{h}_{n_\mathrm{h}}$ can be taken as their average values $\langle n_\mathrm{e}|r_\mathrm{e}|n_\mathrm{e}\rangle$ and $\langle n_\mathrm{h}|r_\mathrm{h}|n_\mathrm{h}\rangle$, respectively. Since $R^\mathrm{e}_{n_\mathrm{e}}$ and $R^\mathrm{h}_{n_\mathrm{h}}$ are approximately equal to each other, $H'_{\mathrm{Q},\lambda,\lambda'}$ would be small. Thus, in the first-order perturbation theory, the total energies and wavefunctions of the exciton with $\omega = 1$ are

$$\begin{aligned}&E(\lambda) = E_\mathrm{R}(n_\mathrm{e}) + E_\mathrm{R}(n_\mathrm{h}) + E_{\mathrm{Qc}}(M) + E_{\mathrm{Qr}}(j) + H'_{\mathrm{Q},\lambda,\lambda}\\ &\Psi_\lambda = \Psi_{R,n_\mathrm{e}}(r_\mathrm{e})\Psi_{R,n_\mathrm{h}}(r_\mathrm{h})\Psi_{\mathrm{Qc},M}(\Theta)\Psi_{\mathrm{Qr},j}(\varphi).\end{aligned} \tag{22}$$

The minimum of $E(n_\mathrm{e}, n_\mathrm{h}, M, 0)$ and proper parameters $\Delta_{n_\mathrm{e},n_\mathrm{h}}$ and $\delta_{n_\mathrm{e},n_\mathrm{h}}$ can be determined by using the variational method. As for a 1D nanoring, the system can be described by taking $n_\mathrm{e} = n_\mathrm{h} \equiv 0$, $R^\mathrm{e}_0 = R^\mathrm{h}_0 = R$ and $\Delta_{0,0} = \sqrt{2}R$ with $H'_\mathrm{Q} = 0$ and $\delta_{0,0} = 1$, and then it can be exactly solved by using the series expansion method introduced earlier [42]. For either the ground or excited state of an exciton confined in a 1D or Q1D nanoring, the binding energy can be defined as the difference in energy of two corresponding levels without ($\omega = 0$) and with ($\omega = 1$) the Coulomb interaction term as

$$E_\mathrm{B}(\lambda) = E(n_\mathrm{e}, n_\mathrm{h}, M, k) - E(n_\mathrm{e}, n_\mathrm{h}, M, j). \tag{23}$$

3. Results and discussion

We take parameters $m^*_\mathrm{e} = 0.067$, $m^*_\mathrm{h} = 0.335$ and $\epsilon_\mathrm{r} = 12.4$ for GaAs materials. The corresponding effective Rydberg Ry^* and effective Bohr radius a^*_B are 5.8 meV and 9.79 nm, respectively. In this section, we will discuss the energy levels and binding energies of an exciton in 1D, Q1D and 2D nanorings with $M = 0$. For the sake of convenience, we define the energy $E_{1(\mathrm{Q})}(M, j)$ as the azimuthal part of $E(\lambda)$ in equation (22) and the corresponding binding energy $E_{\mathrm{B}1(\mathrm{Q})}(M, j)$ as $E_\mathrm{B}(\lambda)$ in equation (23) with $\lambda = \{0, 0, M, j\}$.

First, we would like to obtain proper values of the variational parameters $\Delta_{n_\mathrm{e},n_\mathrm{h}}$ and $\delta_{n_\mathrm{e},n_\mathrm{h}}$. It is found that, as long as the ratio of W to R is small, the energies and $|\langle\lambda'|H'_\mathrm{Q}|\lambda\rangle|$ of ground states with fixed n_e and n_h can reach their minima with almost the same $\Delta_{n_\mathrm{e},n_\mathrm{h}}$ and $\delta_{n_\mathrm{e},n_\mathrm{h}}$. In calculations, we use the variational method to get a set of $\Delta_{n_\mathrm{e},n_\mathrm{h}}$ and $\delta_{n_\mathrm{e},n_\mathrm{h}}$ with

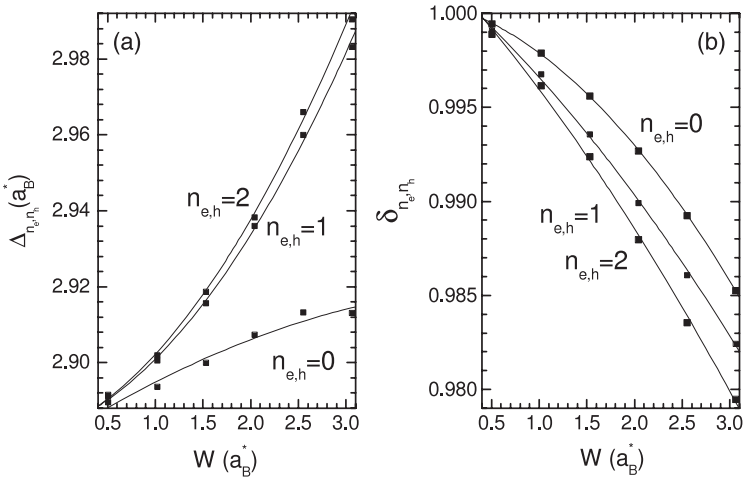

Figure 1. Dependence of (a) Δ_{n_e,n_h} and (b) δ_{n_e,n_h} on W for Q1D nanorings with $R = 2.04\ a_B^*$.

fixed n_e and n_h for different R and W. In figure 1, the dependences of Δ_{n_e,n_h} and δ_{n_e,n_h} with $(n_e, n_h) = (0, 0)$, $(1, 1)$ and $(2, 2)$ on W are shown for Q1D nanorings with $R = 2.04\ a_B^*$ (20 nm). The Δ_{n_e,n_h} are approximately equal to $\sqrt{2}R$ as $W \to 0$ and they increase slowly with W. The δ_{n_e,n_h} are a little smaller than 1 and decrease with increasing W. Although the δ_{n_e,n_h} are very close to that of the 1D nanoring ($\delta_{0,0} = 1$), quite different properties between exciton states in 1D and Q1D nanorings can be found, and this will be discussed below.

3.1. Dimensional effects

In figure 2, we plot the energy levels $E_1(0, j)$ and $E_Q(0, j)$ of an exciton in 1D and Q1D nanorings as functions of R. When R is not very large, the rings with $W/R = 1/2$ are fairly narrow and can be adopted to describe Q1D nanorings. Since the energy of the ground state in a 1D nanoring is negative infinity, we will only concentrate on the excited states. It is easy to note the difference between $E_1(0, j)$ and $E_Q(0, j)$. Because the rotational symmetry in relative motions is destroyed by the attractive Coulomb term, we classify the exciton states into the even and odd states by the symmetry of the wavefunction. As is shown in figure 2(a), $E_1(0, j)$ with energy order j varies greatly with R. As $R \to 0$, $E_1(0, 2k - 1)$ and $E_1(0, 2k)$, corresponding to the even and odd states, approach infinity. As $R \to \infty$, the energy levels converge to those of 1D excitons in which the even and odd states are degenerate. In contrast, in a Q1D nanoring, as shown in figure 2(b), the energy of the ground state only approaches negative infinity as $R \to 0$. The level order of $E_Q(0, j)$ for very small R is the same as that of $E_1(0, j)$; however, with increasing R, crossings between the adjacent energy levels of even and odd states can be found. Marked by the rectangle in figure 2(b) is a crossing between $E_Q(0, 1)$ and $E_Q(0, 2)$ at $R \approx 1.0\ a_B^*$. As $R \to \infty$, the degeneracy between even and odd states does not exist, and the energies of even states are always higher than those of the corresponding odd states. We should note that the sign of the Coulomb interaction term also changes the degeneracy of the even and odd states. For example, the even (singlet) and odd (triplet) states of two electrons in 1D nanorings are split, and the interaction energies increase with node numbers [42].

A remarkable difference can also be found between the binding energies $E_{B1}(0, j)$ and E_{BQ}. In order to better illustrate the behaviour of the binding energies as $R \to 0$, we introduce

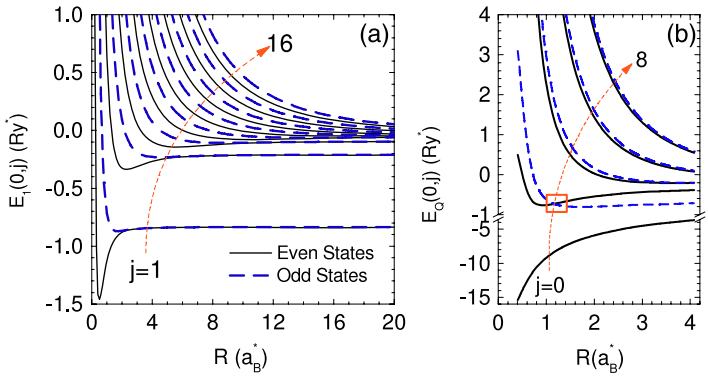

Figure 2. Energy levels $E_1(0, j)$ and $E_Q(0, j)$ of an exciton in 1D (a) and Q1D (b) nanorings versus R, where j is the energy order as shown by the arrow (red). The solid and dashed lines correspond to even and odd states, respectively.

Table 1. Normalized binding energies of an exciton in a 1D nanoring with different R.

	R (a_B^*)	0.1	1.0	5.0	20.0
Even	$\tilde{E}_{B1}(0, 0)$	∞	∞	∞	∞
states	$\tilde{E}_{B1}(0, 1)$	1.028 25	2.330 72	22.185 00	334.683 64
	$\tilde{E}_{B1}(0, 3)$	2.296 48	4.164 09	10.825 85	88.737 86
	$\tilde{E}_{B1}(0, 5)$	3.528 32	5.639 96	14.266 46	49.237 18
	$\tilde{E}_{B1}(0, 7)$	4.749 44	7.032 68	16.899 45	42.827 42
Odd	$\tilde{E}_{B1}(0, 2)$	0.171 40	1.920 26	22.185 00	334.683 64
states	$\tilde{E}_{B1}(0, 4)$	0.214 38	2.216 59	10.564 09	88.737 31
	$\tilde{E}_{B1}(0, 6)$	0.239 75	2.443 49	11.793 18	49.237 17
	$\tilde{E}_{B1}(0, 8)$	0.257 85	2.611 03	12.893 70	42.706 33

the normalized binding energies $\widetilde{E}_{B1(Q)}(0, j) = E_{B1(Q)}(0, j) \cdot R^2$. As shown in figure 3(a) and table 1, $\tilde{E}_{B1}(0, 2k - 1)$ and $\tilde{E}_{B1}(0, 2k)$, corresponding to even and odd states, approach constants and zero, respectively, as $R \to 0$. At the small radius limit, such as $R = 0.1\ a_B^*$, all $\tilde{E}_{B1}(0, 2k - 1)$ are larger than $\tilde{E}_{B1}(0, 2k)$. The characters of the normalized binding energies mentioned above are similar to those of the interaction energies of two electrons [42]. That is to say, the singularity effect of the 1D attractive Coulomb term is much the same as that of the repulsive term as $R \to 0$. However, the R-dependence of the binding energy is quite different from that of interaction energies. The binding energy of the even state, $\tilde{E}_{B1}(0, 2k-1)$, remains larger than that of the odd state, $\tilde{E}_{B1}(0, 2k)$. The difference between $\tilde{E}_{B1}(0, 2k-1)$ and $\tilde{E}_{B1}(0, 2k)$ decreases with increasing R and the corresponding even and odd states approach degeneration as R becomes ever larger. Crossings between $\tilde{E}_{B1}(0, j)$ of even and odd states can appear as R increases from 0 to a finite value. In Q1D nanorings, those characters mentioned above changed greatly due to the absence of singularity in the Coulomb term. As shown in figure 3(b), crossings of binding energies between different states also appear as R varies. Unlike $\tilde{E}_{B1}(0, j)$, the $\tilde{E}_{BQ}(0, j)$ of even states are larger than those of odd states, and all of them approach zero as $R \to 0$.

To better understand the effect of a regular singular point in the Coulomb term, we plot the relative wavefunctions $\Psi_{1r,j}(\varphi)$ and $\Psi_{Qr,j}(\varphi)$ of an exciton in a nanoring with different R

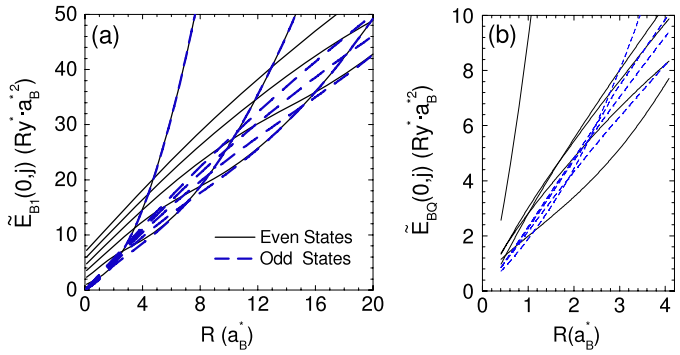

Figure 3. Normalized binding energies of an exciton in (a) 1D and (b) Q1D nanorings as functions of R. The solid and dashed lines correspond to even and odd states, respectively.

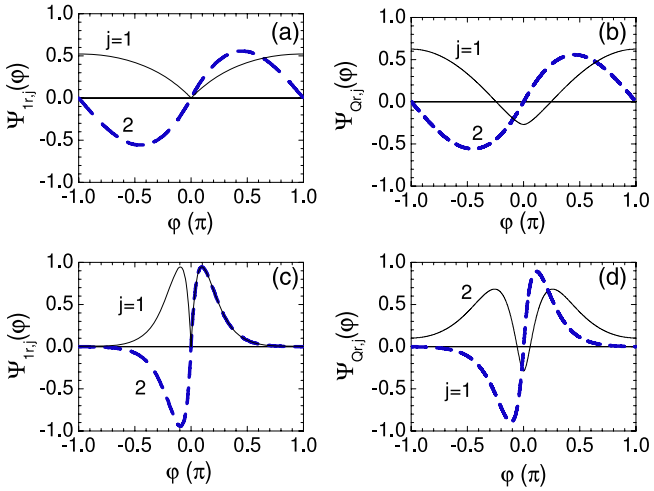

Figure 4. $\Psi_{1r,j}(\varphi)$ of 1D nanorings (a) and $\Psi_{Qr,j}(\varphi)$ of Q1D ones (b) with R equal to 0.4 a_B^*. (c) and (d) are the same as (a) and (b) except $R = 4.0\ a_B^*$. Solid and dashed lines correspond to even and odd states, respectively.

in figure 4. Since M in equation (15) is taken as zero, the periods of $\Psi_{1r,j}(\varphi)$ and $\Psi_{Qr,j}(\varphi)$ are equal to 2π. Then we can choose the region of φ as $[-\pi, \pi)$. It can be seen that $\Psi_{1r,j}(\varphi)$ and $\Psi_{Qr,j}(\varphi)$ of odd states are almost the same. For the same even state, $\Psi_{Qr,j}(\varphi)$ has one more node than $\Psi_{1r,j}(\varphi)$. For small nanorings such as $R = 0.4\ a_B^*$, exciton states mainly depend on the confinement. As shown in figure 4(a), $\Psi_{1r,2}(\varphi)$ has one more node than $\Psi_{1r,1}(\varphi)$, so $E_1(0, 2)$ is higher than $E_1(0, 1)$. In figure 4(b), both $\Psi_{Qr,2}(\varphi)$ and $\Psi_{Qr,1}(\varphi)$ have two nodes, and the difference between $E_Q(0, 2)$ and $E_Q(0, 1)$ is less than that between $E_1(0, 1)$ and $E_1(0, 2)$. However, for large nanorings such as one with $R = 4.0a_B^*$, the attractive Coulomb interaction makes relative wavefunctions of both 1D and Q1D exciton states localize to $\varphi = 0$. In figure 4(c), $\Psi_{1r,1}(\varphi)$ approaches zero at $\psi = \pm\pi$, while $\Psi_{1r,1}(\varphi)$ and $\Psi_{1r,2}(\varphi)$ have almost the same value in $[0, \pi)$, which makes $E_1(0, 1)$ and $E_1(0, 2)$ tend to be degenerate. In figure 4(d), it is easy to note the parity change of $\Psi_{Qr,1}(\varphi)$ and $\Psi_{Qr,2}(\varphi)$, which represents the crossing between $E_Q(0, 1)$ and $E_Q(0, 2)$. $\Psi_{Qr,2}(\varphi)$ has the same number of nodes as $\Psi_{Qr,1}(\varphi)$ and is more extended than $\Psi_{Qr,2}(\varphi)$, so $E_Q(0, 2)$ is larger than $E_Q(0, 1)$.

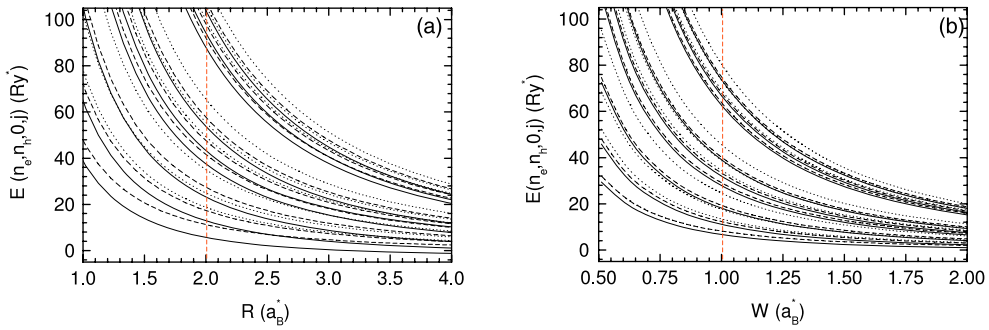

Figure 5. (a) Size effect of $E(n_e, n_h, 0, j)$ for nanorings with $W/R = 1/2$ and (b) shape effect of $E(n_e, n_h, 0, j)$ with $R = 2\ a_B^*$. The solid, dashed and dotted lines correspond to states with $j = 0, 1, 9$.

Table 2. Quantum numbers and orders of $E(n_e, n_h, 0, j)$ for three different nanorings. The underlined letters indicate that orders of corresponding energy levels become lower than those of (2, 1) (a_B^*).

(R, W) (a_B^*)	a: (0, 0, 0), b: (0, 0, 1), c: (0, 1, 0), d: (0, 1, 1), e: (0, 0, 9), f: (0, 2, 0), g: (0, 1, 9), h: (0, 2, 1), i: (0, 2, 9), j: (1, 0, 0), k: (1, 0, 1), l: (1, 1, 0), m: (1, 1, 1), n: (1, 0, 9), o: (1, 2, 0), p: (1, 1, 9), q: (1, 2, 1), r: (1, 2, 9), s: (2, 0, 0), t: (2, 0, 1), u: (2, 1, 0), v: (2, 1, 1), w: (2, 0, 9), x: (2, 2, 0), y: (2, 1, 9), z: (2, 2, 1), ∗: (2, 2, 9)

(2, 1)	a	b	c	d	e	f	g	h	i	j	k	l	m	n	o	p	q	r	s	t	u	v	w	x	y	z	∗
(4, 2)	a	c	b	f	d	e	g	h	j	i	k	l	m	o	n	p	q	r	s	u	t	v	x	w	y	z	∗
(2, 2)	a	c	b	f	d	h	j	l	e	k	m	g	o	q	i	n	s	p	u	t	r	x	v	z	w	y	∗

3.2. Nanorings with different sizes and shapes

Size and shape effects of an exciton in 2D nanorings with finite width are studied by the V–D method. In calculations, we take $n_e, n_h = 1, 2, 3$ and $j = 0$–9 and construct 90 basis functions. Exciton states can be indexed by the quantum numbers (n_e, n_h, M, and j) of their major components. As R varies, the behaviour of $E(n_e, n_h, 0, j)$ with fixed n_e and n_h is similar to that of $E_Q(0, j)$ in a Q1D nanoring. Those crossings between even and odd states obtained by Q1D Hamiltonian still exist in the case of the V–D method. The effect of size and shape on energy levels of an exciton in 2D nanorings is more complex than that in Q1D nanorings. For convenience, we choose $E(n_e, n_h, 0, j)$ with $j = 0, 1, 9$ for each pair of n_e and n_h to study the size and shape effect induced by the radial motions. Figure 5(a) shows the size effect of $E(n_e, n_h, 0, j)$ with $W/R = 1/2$, and figure 5(b) shows the shape effect of $E(n_e, n_h, 0, j)$ with $R = 2\ a_B^*$. As R and W increase, the energies of different states decrease monotonically and crossings between them occur at different positions. To make this clear, we draw a vertical dashed line in both figures 5(a) and (b) which indicates the same nanoring with $R = 2\ a_B^*$ and $W = 1\ a_B^*$. We also list the energy orders and their quantum numbers of exciton states in nanorings with $(R, W) = (2, 1)$, $(4, 2)$ and $(2, 2)$ a_B^* in table 2. The sequence of letters in the first row corresponds to the energy order along the dashed line. Crossings in figure 5(a) are mainly found to be related to $E(n_e, n_h, 0, 0)$ and can be attributed to the competition between the confining potential and the Coulomb interaction. There are more crossings in figure 5(b) because the variation of W not only changes the radial confinement but also changes the Coulomb interaction.

In previous works, the binding energy of an exciton confined in a nanoring was calculated by using a direct diagonalization method [26]; we would like to compare the binding energy

obtained by the V–D method with those obtained by the Q1D variational method and direct diagonalization method. For nanorings with $R = 2.04\ a_B^*$ (20 nm), the binding energies for $W = 0.51, 1.02$ and $3.06\ a_B^*$ obtained by the V–D method are 9.33, 6.29 and 3.60 Ry*, respectively. The corresponding binding energies obtained by the Q1D variational method and direct diagonalization method are 9.21, 6.03, 2.79 Ry*, and 7.33, 5.43, 3.12 Ry* respectively. It can be seen that the Q1D variational method is suitable for rings with W/R smaller than $1/2$.

Based on the discussions above, we can understand the AB oscillations of exciton spectra shown in [28]. In 1D rings, there are no AB oscillations of exciton spectra because the ground-state energy is negative infinity and all wavefunctions of even and odd excited states are equal to zero at $\varphi = 0$. For exciton states in Q1D rings, however, the wavefunction of the ground state is so localized that the oscillator strength is large while the oscillating amplitude is extremely small. Those AB oscillations with small oscillator strengths in the calculated spectra only belong to excited states. In the 2D case, AB oscillations can also be seen in narrow nanorings. In fact, with a very small width, AB oscillations are similar to those in Q1D ones. However, as the ring width increases, radial excitations become much easier, as shown in figure 5, and the oscillator strengths of $E(n_e, n_h, 0, 0)$ with $n_e = n_h$ are quite large. Consequently, their peaks can easily obscure adjacent small AB oscillation peaks. In conclusion, AB oscillations of exciton spectra are most likely to be found in narrow nanorings by experiments with highly sensitive detection techniques.

4. Summary

Using an exact series solution and V–D method, we have studied energy levels and binding energies of an exciton in 1D, Q1D and 2D nanorings. Significant effects of Coulomb interaction on the energy level structure and binding energy of excitons in 1D and Q1D nanorings have been explored. For 1D nanorings with large radii, the even and odd exciton states tend to be degenerate, and the binding energy decreases as the node number increases. Comparing the present work with the case of two-electron states in 1D nanorings, we note that the sign of the Coulomb interaction term can also change the degeneracy of even and odd states. As the radius approaches zero, both the normalized exciton binding energy and two-electron interaction energy increase with increasing node numbers. Moreover, their values approach constants and zero for even and odd states, respectively. In Q1D nanorings, however, the degeneracy of even and odd states at large radius does not exist. Nevertheless, crossings between adjacent energy levels associated with even and odd states are found. In contrast to 1D nanorings, the normalized binding energies of even states become larger than those of odd states, and all of them approach zero as the radius approaches zero. In finite-width nanorings, the variation of radius and width can also change the energy levels and their orders due to the competition between confinement potential and Coulomb interaction. Our study also helps to explain the change of exciton states and their AB oscillation behaviours from 1D to 2D nanorings.

Acknowledgments

Financial support from NSF-China (Grant No. 10374057) and '863' Programme of China is gratefully acknowledged.

Appendix. The V–D method

The Hamiltonian of a few-particle system in a nanostructure is generally written as

$$H = \sum_i H_i + H_{\text{int}}. \tag{A.1}$$

where the H_i are single-particle terms, and H_{int} is the interaction term between different particles. The Hamiltonian H is usually solved by using a diagonalization or variation method. However, in realistic calculations, H_i cannot always be solved directly and H_{int} including attractive Coulomb interaction usually makes the diagonalization process converge slowly. In some cases, a proper trial wavefunction in the variation method is difficult to find.

Considering the disadvantages of linear variation (diagonalization) and Ritz variation methods mentioned above, we combine the two methods together and call the total process the V–D method. In this method, the Hamiltonian H can be reorganized into $N + 1$ parts by variable separation or/and coordinate transform as follows:

$$H = \sum_{j=1}^{N} \mathcal{H}_j(\alpha_j, \beta_j, \gamma_j, \ldots) + \mathcal{H}'. \tag{A.2}$$

Variational parameters $\alpha_j, \beta_j, \gamma_j, \ldots$ are introduced to describe the effective confining potentials and interactions. Eigenenergies $E_j(n_j)$ and eigenfunctions $\Psi_j(n_j, \vec{r}_j)$ of $\mathcal{H}_j(\alpha_j, \beta_j, \gamma_j, \ldots)$ can be obtained by using the series expansion method or other numerical methods. Then a set of variational bases Ψ_λ can be constructed by using $\Psi_j(n_j, \vec{r}_j)$ with $\lambda = \{n_1, n_2, n_3, \ldots, n_N\}$.

$$\Psi_\lambda = F(\Psi_1(n_1, \vec{r}_1), \Psi_1(n_1, \vec{r}_1), \ldots, \Psi_N(n_N, \vec{r}_N)). \tag{A.3}$$

For nonidentical-particle systems such as an exciton, the function F can be simply written as the product of $\Psi_j(n_j, \vec{r}_j)$ with $j = 1$–N. For identical-particle systems such as a few-electron one, F should be exchange-antisymmetric. It should be mentioned that the implementation of the V–D method does not depend on the specific form of F. By defining E_λ and $\mathcal{H}'_{\lambda,\lambda'}$ as

$$\begin{aligned} E_\lambda &= \sum_{j=1}^{N} E_j(n_j) \\ \mathcal{H}'_{\lambda,\lambda'} &= \langle\lambda|\mathcal{H}'|\lambda'\rangle, \end{aligned} \tag{A.4}$$

the V–D process can be described as

$$\begin{aligned} &\sum_{\lambda'} [(E_\lambda - E_i)\delta_{\lambda,\lambda'} + \mathcal{H}'_{\lambda,\lambda'}]A^i_{\lambda'} = 0, \\ &E_{\text{g}} = \min_{\{v_1, v_2, \ldots, v_N\}} E_0, \end{aligned} \tag{A.5}$$

and the detailed description using Newton's method is as follows.

(1) Initialize the parameters $\{v_1, v_2, \ldots, v_N\}$.
(2) Solve $\{E_j(n_j), \Psi_j(n_j, \vec{r}_j)\}$ and construct the variational bases Ψ_λ.
(3) Diagonalize the Hamiltonian matrix: $\sum_{\lambda'}[(E_\lambda - E_i)\delta_{\lambda,\lambda'} + \mathcal{H}'_{\lambda,\lambda'}]A^i_{\lambda'} = 0$.
(4) Calculate the gradient of E_0, adjust the parameters and jump to step (2) until the gradient reaches zero.
(5) Finally, obtain the ground-state energy: $E_{\text{g}} = \min_{\{v_1, v_2, \ldots, v_N\}} E_0$.

Here E_i is the eigenenergy and $A^i_{\lambda'}$ is the expansion coefficient of the eigenwavefunction, v_j represents a set of variational parameters $\{\alpha_j, \beta_j, \gamma_j, \ldots\}$. It is obvious that the E_0 are dependent on the variational parameters $\alpha_j, \beta_j, \gamma_j, \ldots$ with j from 1 to N. The ground-state energy E_{g} and the excited-state energies as well as the corresponding basis can be obtained simultaneously by finding the minimum of E_0 with the proper parameters.

It should be noted that parameters introduced in $\mathcal{H}_j(\alpha_j, \beta_j, \gamma_j, \ldots)$ can be easily chosen in expressions of effective confining potentials and interactions. If the ring is not very wide, the matrix elements $\mathcal{H}'_{\lambda,\lambda'}$ with proper parameters are usually small, and hence the diagonalization

process converges quickly and a small number of basis functions are needed. Even for rings with large width, the V–D method converges much faster than direct diagonalization. For example, the ground-state energy E_g of an exciton in a nanoring with $R = W = 20$ nm obtained by using 90 variational basis functions converges better than that by using 256 usual functions constructed by single-carrier orbitals.

References

[1] Garcia J M, Medeiros Ribeiro G, Schmidt K, Ngo T, Feng J L, Lorke A, Kotthaus J and Petroff P M 1997 *Appl. Phys. Lett.* **71** 2014
[2] Garcia J M, Silveira J P and Briones F 2000 *Appl. Phys. Lett.* **77** 409
[3] Lorke A, Luyken R J, Govorov A O, Kotthaus J P, Garcia J M and Petroff P M 2000 *Phys. Rev. Lett.* **84** 2223
[4] Lorke A, Luyken R J, Garcia J M and Petroff P M 2001 *Japan. J. Appl. Phys.* **40** 1857
[5] Warburton R J, Schaflein C, Haft D, Bickel F, Lorke A, Karrai K, Garica J M, Schoenfeld W and Petroff P M 2000 *Nature* **405** 926
[6] Pettersson H, Warburton R J, Lorke A, Karrai K, Kotthaus J P, Garica J M and Petroff P M 2000 *Physica* E **6** 510
[7] Warburton R J, Schaflein C, Haft D, Bickel F, Lorke A, Karrai K, Garica J M, Schoenfeld W and Petroff P M 2001 *Physica* E **9** 124
[8] Haft D, Schulhauser C, Govorov A O, Warburton R J, Karrai K, Garcia J M, Schoenfeld W and Petroff P M 2002 *Physica* E **13** 165
[9] Bayer M, Korkusinski M, Hawrylak P, Gutbrod T, Michel M and Forchel A 2003 *Phys. Rev. Lett.* **90** 186801
[10] Hu H, Zhu J L and Xiong J J 2000 *Phys. Rev.* B **62** 16777
[11] Emperador A, Pi M, Barranco M and Lorke A 2000 *Phys. Rev.* B **62** 4573
[12] Barticevic Z, Pacheco M and Latge A 2000 *Phys. Rev.* B **62** 6963
[13] Puente A and Serra L 2001 *Phys. Rev.* B **63** 125334
[14] Li S S and Xia J B 2001 *J. Appl. Phys.* **89** 3434
[15] Voskoboynikov O, Li Y M, Lu H M, Shih C F and Lee C P 2002 *Phys. Rev.* B **66** 155306
[16] Barticevic Z, Fuster G and Pacheco M 2002 *Phys. Rev.* B **65** 193307
[17] Llorens J M, Trallero-Giner C, Garcia-Cristobal A and Cantarero A 2001 *Phys. Rev.* B **64** 035309
[18] Lavenere-Wanderley L A, Bruno-Alfonso A and Latge A 2002 *J. Phys.: Condens. Matter* **14** 259
[19] Xia J B and Li S S 2002 *Phys. Rev.* B **66** 035311
[20] Planelles J, Jaskolski W and Aliaga J I 2002 *Phys. Rev.* B **65** 033306
[21] Bruno-Alfonso A and Latge A 2000 *Phys. Rev.* B **61** 15887
[22] Chaplik A V 1995 *JETP Lett.* **62** 900
[23] Romer R A and Raikh M E 2000 *Phys. Status Solidi* b **221** 535
[24] Romer R A and Raikh M E 2000 *Phys. Rev.* B **62** 7045
[25] Pereyra P and Ulloa S E 2000 *Phys. Rev.* B **61** 2128
[26] Song J and Ulloa S E 2001 *Phys. Rev.* B **63** 125302
[27] Maschke K, Meier T, Thomas P and Koch S W 2001 *Eur. Phys. J.* B **19** 599
[28] Hu H, Zhu J L, Li D J and Xiong J J 2001 *Phys. Rev.* B **63** 195307
[29] Hu H, Zhang G M, Zhu J L and Xiong J J 2001 *Phys. Rev.* B **63** 045320
[30] Ulloa S E, Govorov A O, Kalameitsev A V, Warburton R and Karrai K 2002 *Physica* E **12** 790
[31] Galbrath I, Braid F J and Warburton R J 2002 *Phys. Status Solidi* a **190** 781
[32] Maslov A V and Citrin D S 2003 *Phys. Rev.* B **67** 121304(R)
[33] Climente J I, Planelles J and Jaskolski W 2003 *Phys. Rev.* B **68** 075307
[34] Zhang T Y and Cao J C 2005 *J. Appl. Phys.* **97** 024307
[35] DiasdaSilva L G G V, Ulloa S E and Govorov A O 2004 *Phys. Rev.* B **70** 155318
[36] Govorov A O, Ulloa S E, Karrai K and Warburton R J 2002 *Phys. Rev.* B **66** 081309(R)
[37] Ribeiro E, Govorov A O, Carvalho W and Medeiros-Ribeiro G 2004 *Phys. Rev. Lett.* **92** 126402
[38] Hu H, Li D J, Zhu J L and Xiong J J 2000 *J. Phys.: Condens. Matter* **12** 9145
[39] Szafran B, Adamowski J and Bednarek S 2002 *J. Phys.: Condens. Matter* **14** 73
[40] DiasdaSilva L G G V, Ulloa S E and Shahbazyan T V 2005 *Phys. Rev.* B **72** 125327
[41] Barticevic Z, Pacheco M, Simonin J and Proetto C R 2005 *Phys. Rev.* B **73** 165311
[42] Zhu J L, Dai Z S and Hu X 2003 *Phys. Rev.* B **68** 045324